Redondo Beach, CA 90278

TRW

AD-A141 877

12

DTIC FILE COPY

DTIC
ELECTE
JUN 0 6 1984
S D
E

This document has been approved for public release and sale; its distribution is unlimited.

84 06 04 012

12

37564-6002-UT-00

THE NATURE OF MICROWAVE BACKSCATTERING FROM WATER WAVES

by

DANIEL S. W. KWOH
BRUCE M. LAKE

MAY 1984

Prepared for

Office of Naval Research
Coastal Sciences Program
Contract No. N00014-C-81-0217

APPROVED FOR PUBLIC RELEASE, DISTRIBUTION UNLIMITED

TRW SPACE AND TECHNOLOGY GROUP
ONE SPACE PARK
REDONDO BEACH, CALIFORNIA 90278

UNCLASSIFIED

SECURITY CLASSIFICATION OF THIS PAGE (When Data Entered)

REPORT DOCUMENTATION PAGE		READ INSTRUCTIONS BEFORE COMPLETING FORM
1. REPORT NUMBER TRW Report No. 37564-6002-UT-00	2. GOVT ACCESSION NO. AD-A147 947	3. RECIPIENT'S CATALOG NUMBER
4. TITLE (and Subtitle) The Nature of Microwave Backscattering from Water Waves		5. TYPE OF REPORT & PERIOD COVERED Final, 10-1-82 to 10-1-83
		6. PERFORMING ORG. REPORT NUMBER
7. AUTHOR(s) Daniel S. W. Kwoh Bruce M. Lake		8. CONTRACT OR GRANT NUMBER(s) N00014-81-C-0217
9. PERFORMING ORGANIZATION NAME AND ADDRESS Fluid Mechanics Department TRW Space and Technology Group, One Space Park, Redondo Beach, CA 90278		10. PROGRAM ELEMENT, PROJECT, TASK AREA & WORK UNIT NUMBERS
11. CONTROLLING OFFICE NAME AND ADDRESS Office of Naval Research Coastal Sciences Program Arlington, VA 22217		12. REPORT DATE May 1984 13. NUMBER OF PAGES 32
14. MONITORING AGENCY NAME & ADDRESS(if different from Controlling Office)		15. SECURITY CLASS. (of this report) Unclassified 15a. DECLASSIFICATION/DOWNGRADING SCHEDULE

16. DISTRIBUTION STATEMENT (of this Report)

Approved for public release; distribution unlimited

17. DISTRIBUTION STATEMENT (of the abstract entered in Block 20, if different from Report)

18. SUPPLEMENTARY NOTES

19. KEY WORDS (Continue on reverse side if necessary and identify by block number)

Microwave Backscattering
Deep-Water Gravity Waves

20. ABSTRACT (Continue on reverse side if necessary and identify by block number)

Our recent laboratory study shows that Bragg scattering by itself is not an adequate description for microwave backscattering from water waves. It may account for part of the scattering, but reflection from specular facets and wedge-like diffractive scattering from small radius crests of waves can predominate.

Our first experiment was performed on wave paddle-generated short gravity waves. Using a scanning laser slope gauge to measure the surface and the moments

DD FORM 1 JAN 73 1473 EDITION OF 1 NOV 65 IS OBSOLETE

(Cont. on reverse side)

UNCLASSIFIED

SECURITY CLASSIFICATION OF THIS PAGE (When Data Entered)

method to compute the scattering, we found that the small radius crests of such waves can be the more dominant source of scattering and that the description of such scattering is closer to wedge diffraction than Bragg scattering. Bragg scattering does describe the scattering from the parasitic capillaries. We also found that specular reflection is more important than generally expected.

Our second experiment was performed on wind waves. We found that at low wind, the Doppler spectrum is narrow peaked but it gradually evolves to become a doubly peaked spectrum at high wind. Analysis shows that low wind scattering is indeed Bragg scattering. At high wind, the lower frequency peak again is due to Bragg scattering from rough patches, whereas the higher frequency peak is due to scattering from waves not unlike the paddle-generated short gravity waves.

TABLE OF CONTENTS

Acknowledgement

The authors would like to thank Peter Lee for leaving us a radar system that works, Dewey Rowland, Rudy Acosta, Brian McGee, and Ernie Hoover for assistance in the course of the work, Jim Sherman for designing the slope gauge electronics, Dick Wagner for first lending us his laser slope gauge and later helping us to modify it into the scanning version, and Hans Dolezalek for encouragement and critical comments.

Abstract

Our recent laboratory study shows that Bragg scattering by itself is not an adequate description for microwave backscattering from water waves. It may account for part of the scattering, but reflection from specular facets and wedge-like diffractive scattering from small radius crests of waves can predominate.

Our first experiment was performed on wave paddle-generated short gravity waves. Using a scanning laser slope gauge to measure the surface and the moments method to compute the scattering, we found that the small radius crests of such waves can be the more dominant source of scattering and that the description of such scattering is closer to wedge diffraction than Bragg scattering. Bragg scattering does describe the scattering from the parasitic capillaries. We also found that specular reflection is more important than generally expected.

Our second experiment was performed on wind waves. We found that at low wind, the Doppler spectrum is narrow peaked but it gradually evolves to become a doubly peaked spectrum at high wind. Analysis shows that low wind scattering is indeed Bragg scattering. At high wind, the lower frequency peak again is due to Bragg scattering from rough patches, whereas the higher frequency peak is due to scattering from waves not unlike the paddle-generated short gravity waves.

EXECUTIVE SUMMARY

Our recent laboratory study shows that Bragg scattering by itself is not an adequate description for microwave backscattering from water waves. It may account for part of the scattering, but reflection from specular facets and wedge-like diffractive scattering from small radius crests of waves can predominate.

Our first experiment was performed on wave paddle-generated short gravity waves. Using a scanning laser slope gauge to measure the surface and the moments method to compute the scattering, we found that the small radius crests of such waves can be the more dominant source of scattering and that the description of such scattering is closer to wedge diffraction than Bragg scattering. Bragg scattering does describe the scattering from the parasitic capillaries. We also found that specular reflection is more important than generally expected.

Our second experiment was performed on wind waves. We found that at low wind, the Doppler spectrum is narrow peaked but it gradually evolves to become a doubly peaked spectrum at high wind. Analysis shows that low wind scattering is indeed Bragg scattering. At high wind, the lower frequency peak again is due to Bragg scattering from rough patches, whereas the higher frequency peak is due to scattering from waves not unlike the paddle-generated short gravity waves.

Our conclusions regarding the nature of microwave backscatter from water waves based on these laboratory measurements can be summarized as follows:

1. Electromagnetically, we have identified three sources for microwave backscattering from water waves:
   - (i) specular reflection from turbulent wakes or steep capillaries
   - (ii) rounded wedge diffraction from sharp crests of waves
   - (iii) Bragg scattering from parasitic capillaries or turbulent patches.
2. Hydrodynamically, we have identified three sources for wind-wave scattering: low wind free waves, high wind bound waves and turbulent patches.

3. We now have explanations for

   (i) the evolution of the Doppler spectrum with increasing wind

   (ii) the width of the Doppler spectrum

   (iii) the location of peak(s) of the Doppler spectrum

   (iv) the asymmetry of the Doppler spectrum.

4. The implications for microwave backscattering from ocean waves are:

   (i) specular reflection at low θ_i (e.g., 20°) may be much more important than generally expected

   (ii) the relative frequency of occurrence of specular facets, sharp crests and turbulent patches will determine the character of ocean scattering, both for incident angle and frequency selection and for determination of modulation transfer functions.

I. INTRODUCTION

During the past ten years, the "composite model" has become increasingly accepted as the correct theory for the description of microwave scattering from the ocean surface. The basic premise of the theory is that microwave radiation (at moderate to large incidence angles) backscatters from "slightly rough" patches which are created by wind on the ocean surface. These patches are geometrically tilted by the underlying gravity waves and they also interact dynamically with the wind, the wind drift layer and the orbital current of underlying gravity waves. The electromagnetic theory that describes the scattering mechanism was developed by Rice[1]. The microwave radiation is assumed to scatter selectively from a Fourier component of the "slightly rough" surface which satisfies the Bragg condition. The theory that describes the interaction between this Bragg component and other wave components and currents and wind has gone through various stages of development to reach its present rather elaborate form as described by Hasselmann[2] and Wright et al[3].

When we started our investigation of microwave scattering from water waves, it seemed quite unsatisfactory to us that despite the widespread conviction that "Bragg waves" are doing the scattering, there was no clear concept of what the "Bragg waves" actually are. Are they really corrugation-like wavelets or ripples on a windblown surface, or are they a Fourier component in a random rough patch? Or could they be a Fourier component of a fairly sharp crest? To answer these questions, the obvious thing to do would be to examine a scattering surface in great detail and see what it is actually like when scattering is taking place.

Our experience in the study of the dynamics of deep-water waves encouraged us to consider the usefulness and feasibility of a deterministic approach. Initial studies further convinced us that it is both warranted and feasible to perform quantitative and deterministic water wave and microwave measurements to identify the relative contributions of specific surface features to total backscattering. More specifically, we attempted to measure the exact surface profile while microwave scattering is taking place. In the laboratory, we focused our attention first on short gravity waves generated by a wave paddle rather than on wind waves. The wave paddle generated waves are less random, more long-crested and yet exhibit certain characteristics similar to wind waves. They are therefore a logical first

step for a deterministic study. With the wave profiles measured, we solved for the scattering by a numerical method and compared the computed results with the measured results. Using numerical modeling, we identified scattering contributions of different surface features. Next, we studied wind-generated waves using a similar approach. The experimental setup and procedures, numerical procedure, and final results are discussed in greater detail in the following sections.

II. EXPERIMENTAL SETUP

The experiment was performed in a wave tank which is 12 m long and 92 cm wide. The tank is filled to a depth of 90 cm with distilled water. There is an open-circuit wind tunnel with a cross section of 122 cm x 92 cm on top of the wave tank. The inside surface of the wind tunnel is completely covered with 40 db microwave absorbing material. Water waves are generated either by a wave paddle at one end of the tank or by wind and propagate to the other end where they are absorbed by a shallow-angle beach.

The x-band radar system is a 9.23 GHz (3.248 cm) cw superheterodyne coherent system with roughly 100 mw transmitted power and dual transmitting and receiving channels, each of which provides individual phase and amplitude (i.e., linear detection) outputs. Each channel can be individually nulled to cancel background stray reflections. The antenna is a corrugated, conical horn with a 22.9 cm aperture fitted with a matched dielectric lens with a focal length of 45.7 cm. The 3-db beamwidths are 8.48 cm and 8.43 cm for vv and hh polarization respectively at the focal plane.

To measure an almost instantaneous profile of the water surface while microwave scattering is taking place, we have developed a scanning laser slope gauge (SLSG) which is a natural extension of the laser slope gauge first developed by Wagner et al.[4] The laser slope gauge provides a noninterfering, co-located simultaneous measurement of the surface with good spatial resolution and frequency response. However, the slope gauge observes what is happening at one point whereas the microwave radar is observing a large area. To remedy the situation, we implemented scanning of the laser beam so that it scans the water surface in the direction of wave propagation over 13.3 cm at 39.063 Hz. The detected output thus provides an almost instantaneous slope profile of the surface at close to 40 times/sec. The angular range of the SLSG is about 60° which can be offset in either direction. With calibration, the slope gauge has an accuracy of ± 0.3°, so that it can be meaningfully integrated to provide the displacement profile.

Besides the SLSG, another optical sensor was deployed to monitor the presence of specular facets at an angle normal to the microwave incidence the water surface. This is accomplished by putting a projector lamp to one side of the corrugated horn and a camera with a zoom lens to the other side.

Both the projector lamp and the zoom lens are aimed at the patch of surface under microwave illumination and both are set at the same angle as the horn. A large circular photodiode detector is placed at the film plane of the camera whose shutter is left open. After amplification, the output of the detector shows spikes whenever specular facets appear in the field of view of the camera. This is our criterion for separating the "nonspecular" from the "specular" scattering events.

For comparison purposes, a capacitance level gauge was also installed close to the side of the wave tank.

Figure 1 shows a schematic arrangement of the SLSG together with the corrugated horn inside the wind tunnel-wave tank.

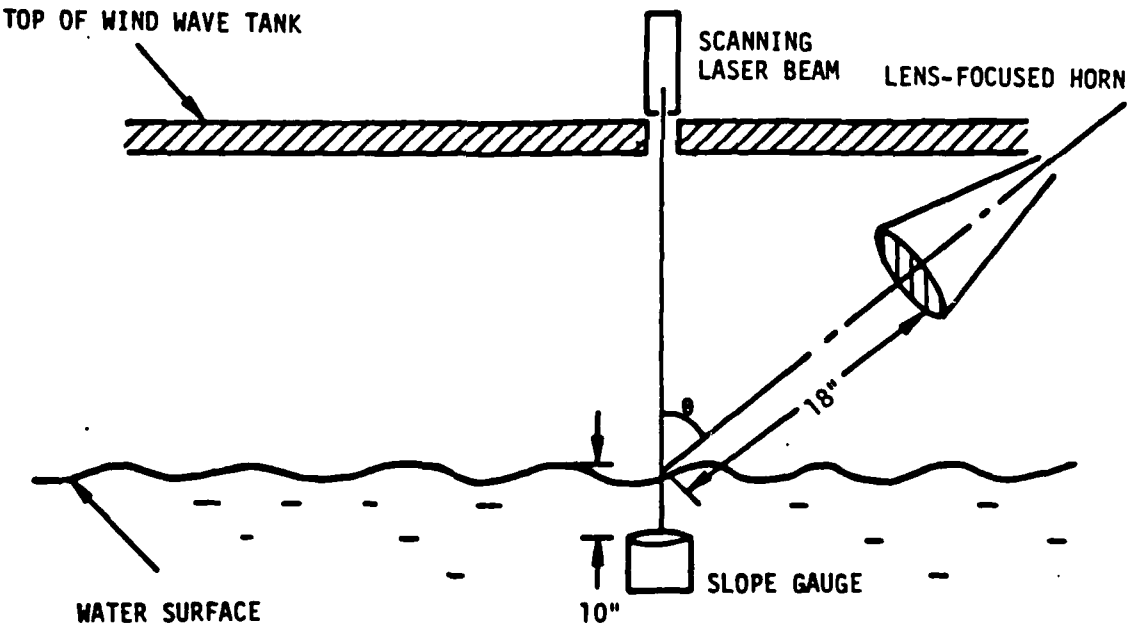

Figure 1.

III. EXPERIMENTAL APPROACH

We first studied the simpler wave system, the mechanically-generated short gravity waves with frequency of 2.5 Hz ($\sim$ 25 cm) and amplitude $\sim$ 1 cm ($ka \sim 0.17$). Microwave backscattering amplitude and phase for both vv and hh polarizations were measured for 40°, 55° and 70° incidence angles.

First, specular scattering events were separated from the nonspecular events by the use of the specular reflection sensor. Pictures were taken to identify the origin of the specular facets responsible for this kind of scattering.

Completely nonspecular events were analyzed in a deterministic fashion. The scanned slope profiles were first recorded. The moments methods was then applied using the slope profiles and the measured antenna pattern to compute the induced surface electromagnetic current and the complex scattering amplitudes in all directions, including the backscattering direction. The computed backscattering amplitude, amplitude polarization ratio and phase were then compared with the measured values to validate both our experimental and numerical procedures. Once this was accomplished, numerical modeling was performed to determine which features on the water surface contribute significantly to the scattering and which approximate theories best describe the scattering from particular surface features.

For wind-wave scattering, a similar approach was taken. In addition, the Doppler spectrum was also measured. The task was to understand the shape and evolution of the Doppler spectrum with increasing wind speed as a function of the evolution of the water surface with increasing wind speed. The scattering signatures of different features that we identified in the mechanical wave scattering measurements were applied to the interpretation of wind-wave scattering.

IV. BACKSCATTERING FROM MECHANICALLY-GENERATED WAVES

An example of backscattering from mechanically-generated short gravity waves at $\theta_i = 55°$ is shown in Figure 2. Trace 1 is the output of the laser slope gauge operating in its stationary mode. Trace 2 is the displacement of the water surface as measured by the capacitance gauge. Traces 3 and 4 are the absolute amplitudes in vv and hh. Trace 5 is the phase of the vv channel. Several interesting features can be noticed immediately: (i) the parasitic capillaries generated during wavebreaking are easily discernible in the slope gauge output but not the capacitance level gauge output; (ii) microwave backscattering occurs in a burst almost coincident with the wavebreaking; (iii) vv amplitude is bigger than hh and its ratio can be easily measured; (iv) the number of cycles/sec in the phase channel is the Doppler shift. Our task is to understand the backscattering (as shown in traces 3, 4, 5) in terms of the surface (as shown in traces 1 and 2). This requires scanning the laser slope gauge to obtain an almost instantaneous surface profile. Figure 3(a) shows an example of a scanned slope profile. It is integrated to give the displacement profile. The moments method is applied to compute the scattered power for both the TE mode (vv) and TM mode (hh) [Figure 3(b)]. This procedure is performed for about 40 events for each angle $\theta_i = 40°$, 55° and 70°.

Figure 4 shows a comparison between measured absolute power for both polarizations and $\theta_i = 40°$, 55° and 70°. The solid line is a calibration obtained from standard two-dimensional target scattering measurements. It can be seen that measured power is proportional to computed power over ~ 30 db, but smaller by ~ 4 db over the whole range. This is probably because the width of the scattering region is less than the antenna beamwidth. Figure 5 shows that the computer polarization ratio agrees quite well with the measured ratios over the 3 incidence angles. Figure 6 shows the computed Doppler shift vs. the measured Doppler shift. The computed Doppler shift is arrived at by computing the scattering from successive scans. Again, the agreement is quite good over all three incidence angles. We have thus shown that with careful measurements and correct computations, microwave backscattering from mechanically-generated water waves can be accounted for in an exact manner.

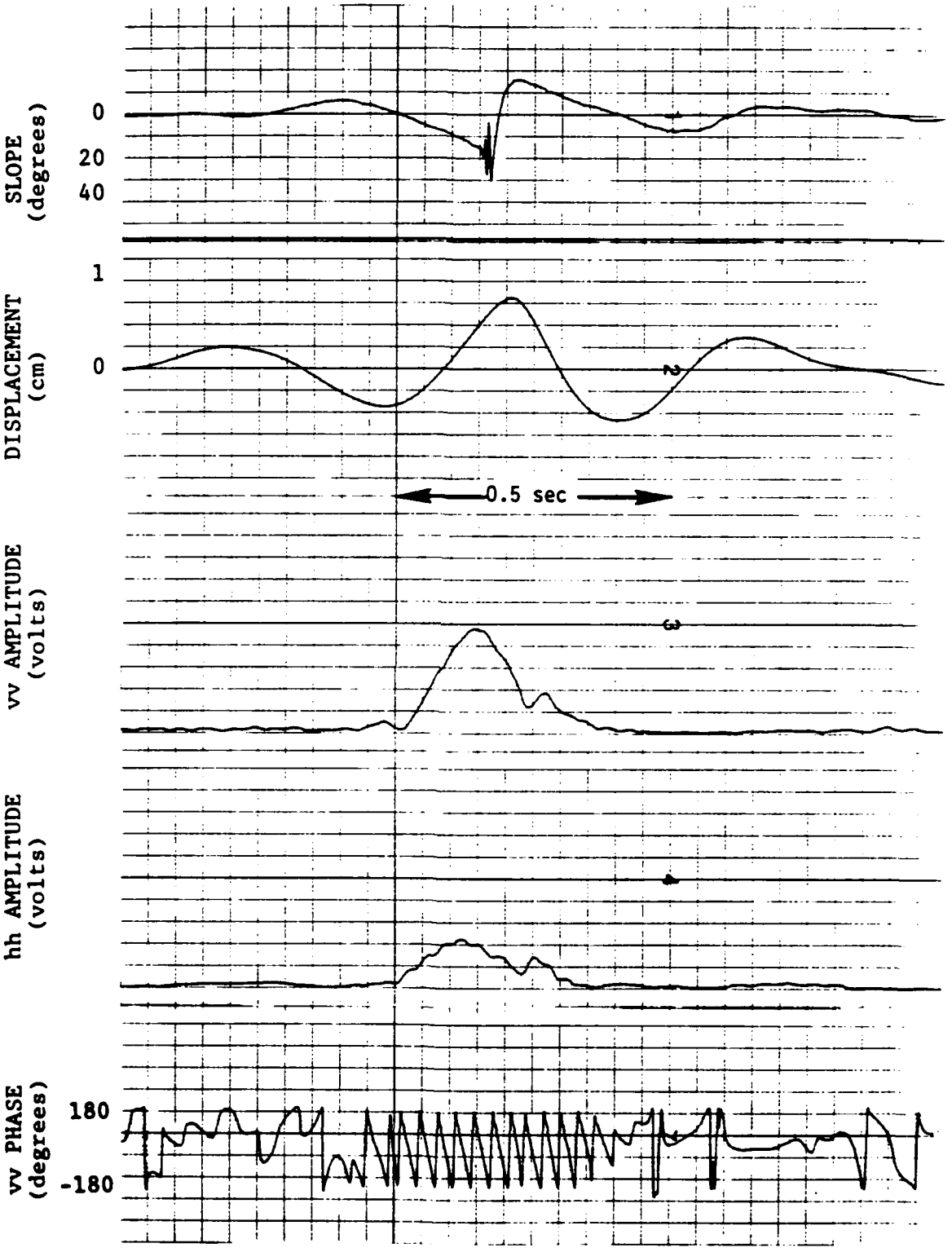

Figure 2. Backscattering from mechanically-generated short gravity waves.

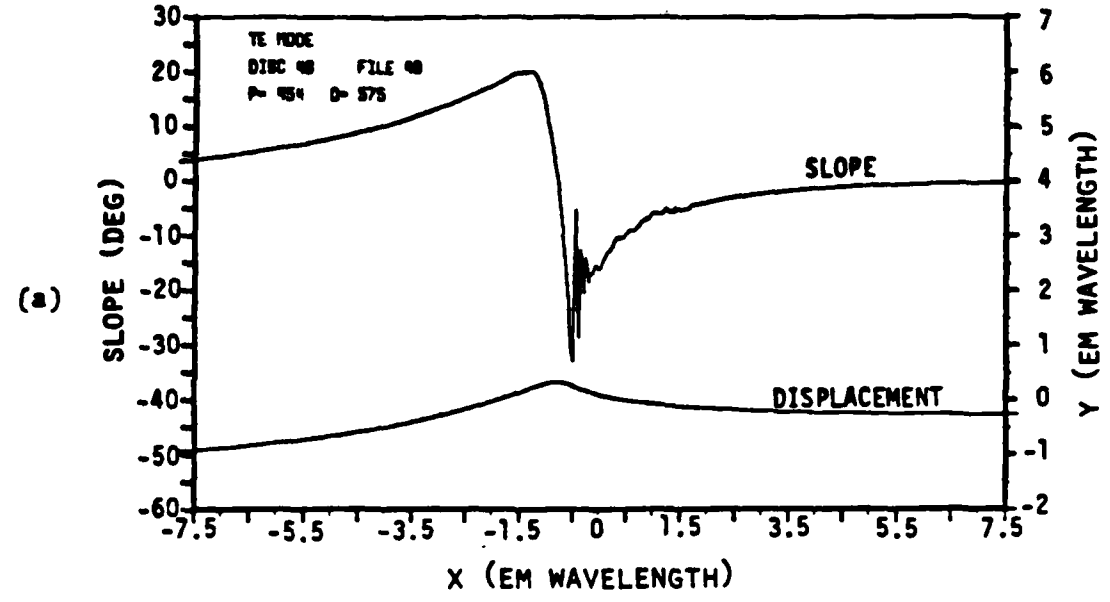

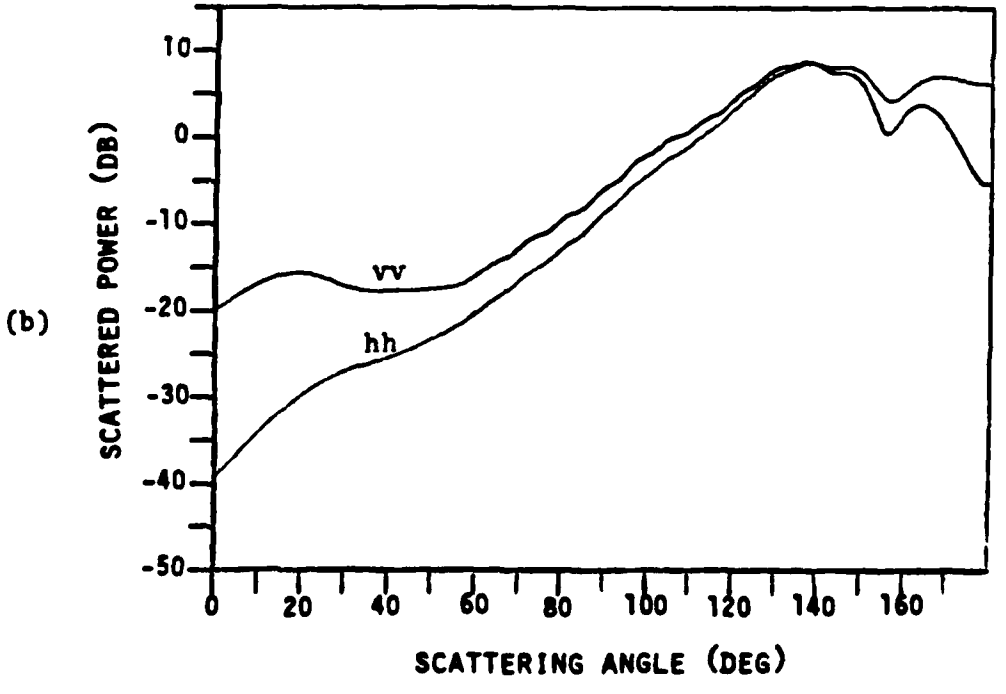

Figure 3. (a) Slope and displacement profile of event in a scan.
(b) vv and hh scattered power ($\equiv 20 \log_{10}|E_z^s|$) as a function of angle as computed by moments method.

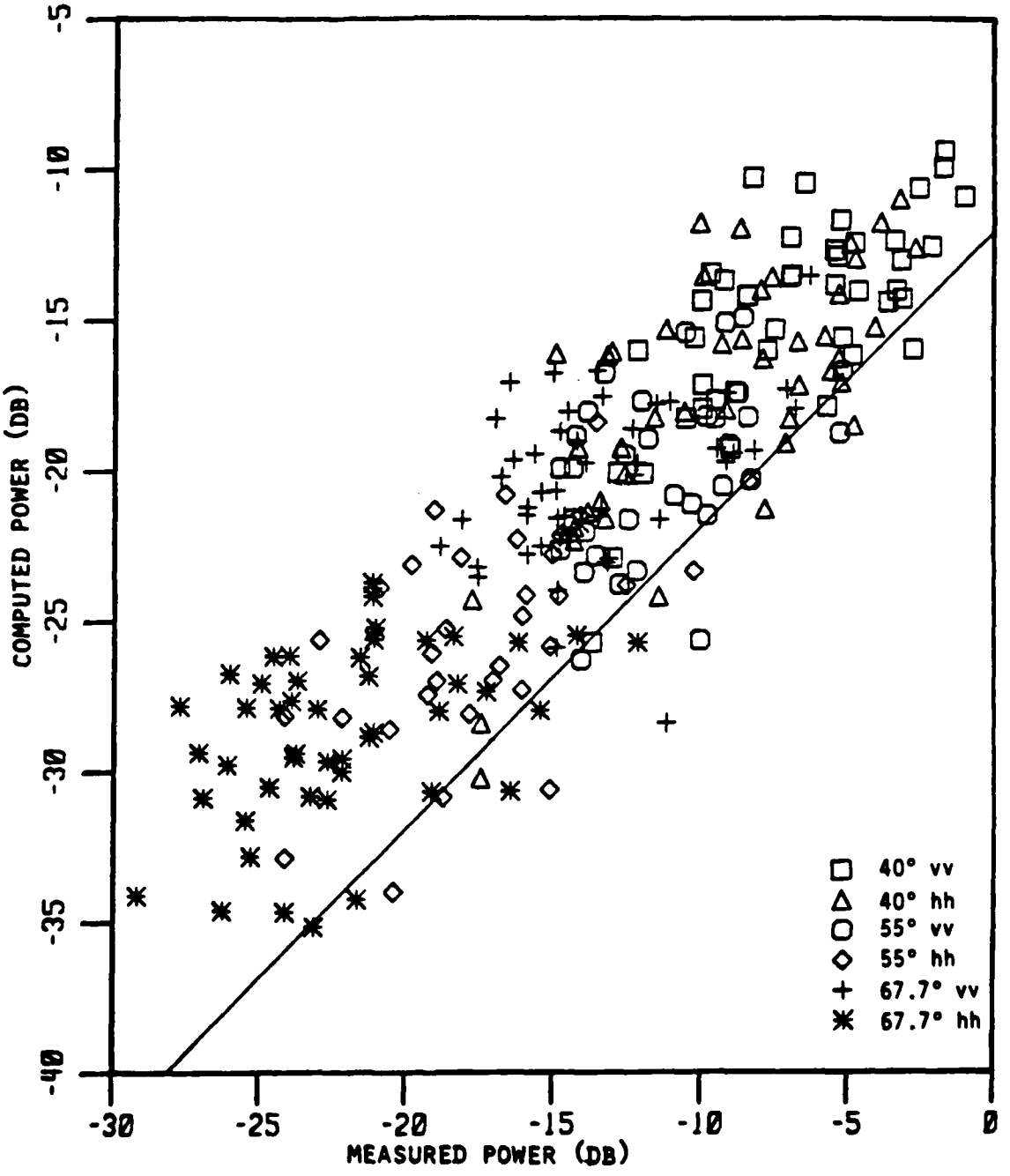

Figure 4. Computed power (by moments method) vs. measured power in vv and hh polarizations for 40°, 55°, 67.7° incidence angles. Solid line is calibration line.

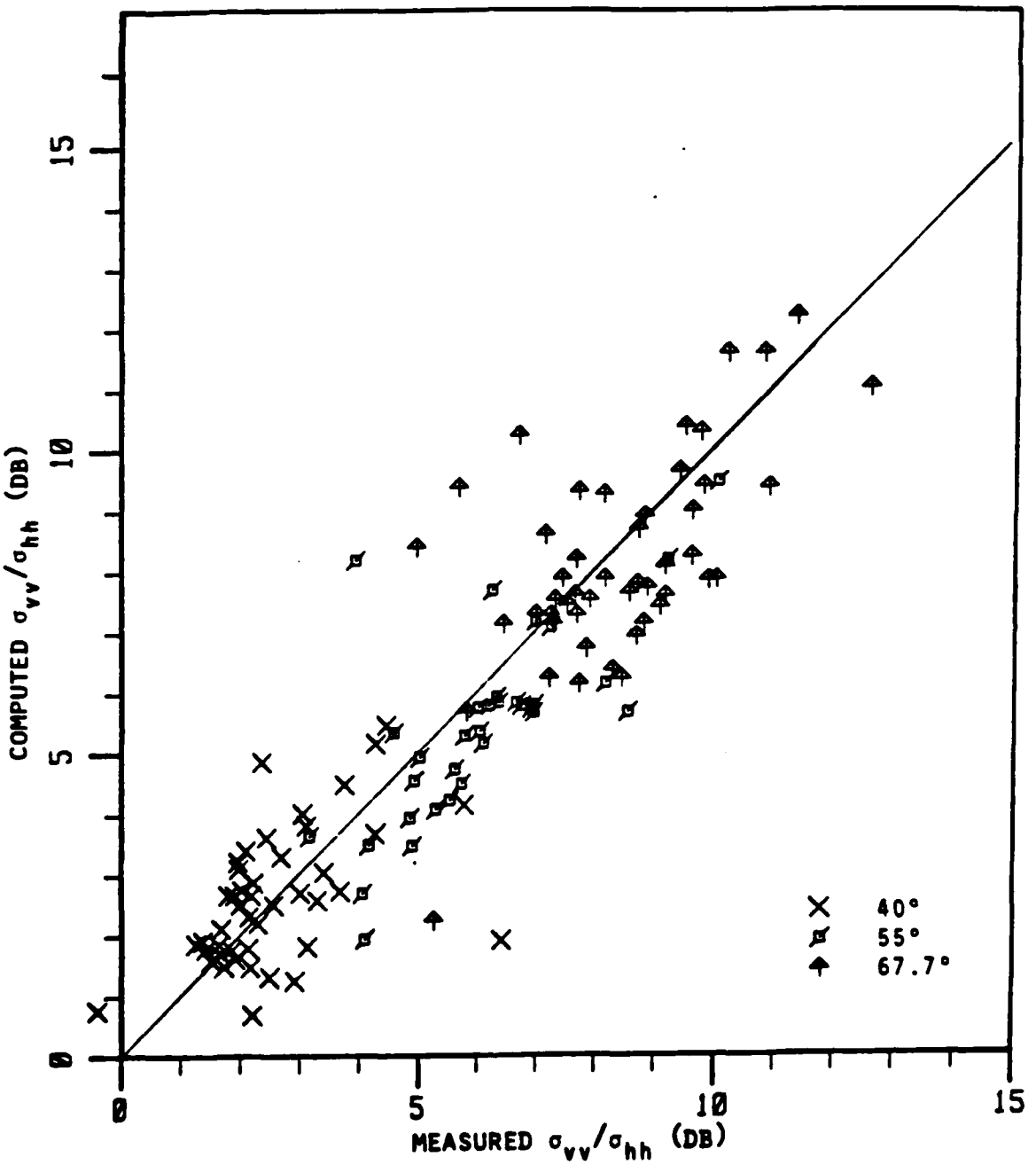

Figure 5. Computed polarization ratio (by moments method plus small perturbation correction for water being a dielectric) vs. measured polarization ratio for backscattering at 40°, 55° and 67.7°. Solid line is 45° line.

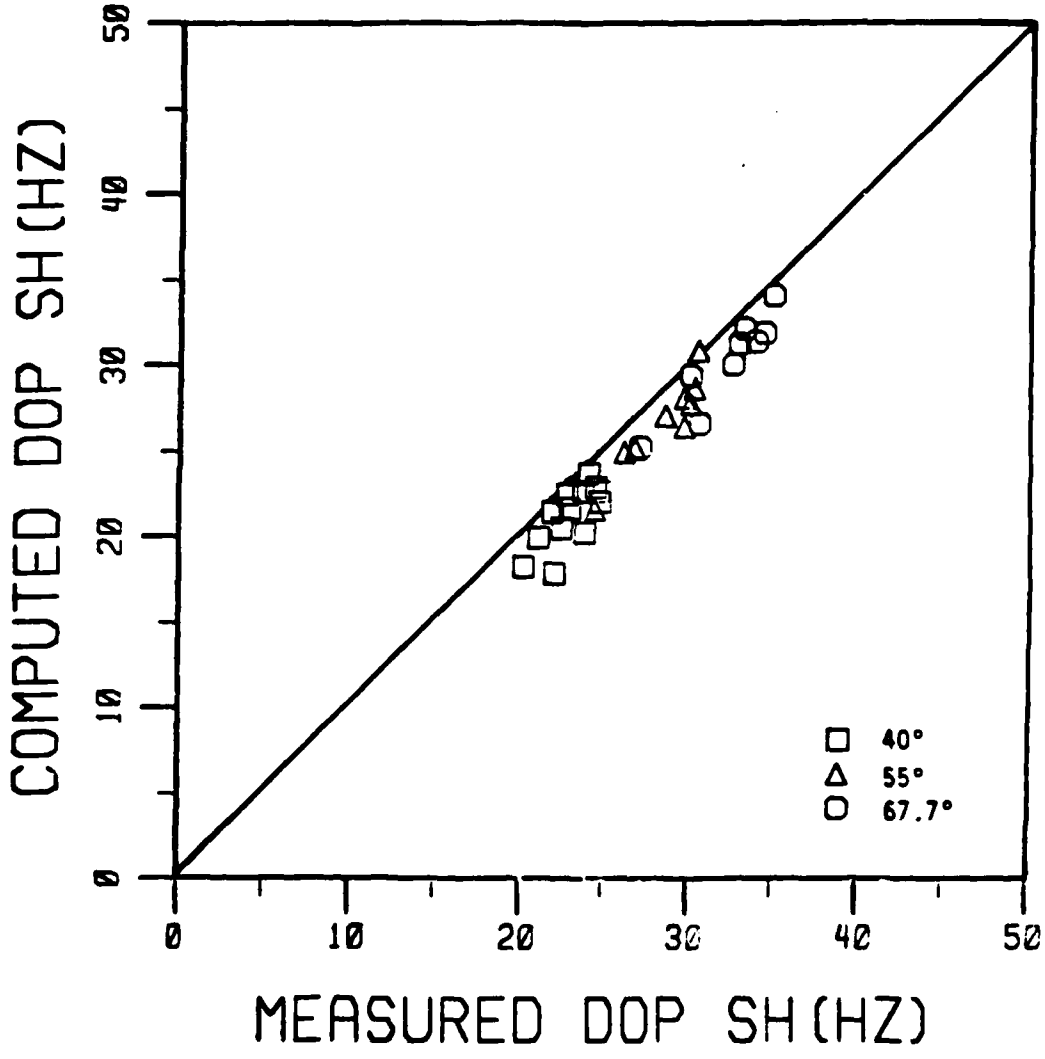

Figure 6. Computed Doppler shift vs. measured Doppler shift for backscattering events at 40°, 55°, 67.7° from 2.5 Hz wavetrains. The solid line is the 45° line.

We are now justified in doing numerical modeling. For example, scattering from the previously shown slope profile [Figure 3(a)] can be thought of as the direct sum of scattering from the capillary waves (put on an inclined plane) and scattering from the wave with capillaries smoothed away. Figure 7(a) shows the resultant scattering. With the capillary waves smoothed away, the small radius crest region is the only high frequency feature left and scatters like a rounded wedge. It can be shown that the scattering in this case is not describable by small perturbation theory, i.e., it is not Bragg scattering. A more appropriate description may be wedge diffraction (as in Geometric Theory of Diffraction), slightly modified to account for the rounded tip. For the capillary waves, the small perturbation prediction agrees with the moments method computation [Figures 8 and 9]. This implies that the scattering from capillary waves is "Bragg scattering".

So far, we have concentrated on nonspecular scattering. There is occasionally specular reflection from small facets which are steep enough to be normal to the microwave incidence direction. Figure 10 shows examples of such specular facets. They are either very steep capillaries or are in the turbulent wake behind a breaking wave. When specular reflection occurs, one good indication (other than the specular reflection sensor) is that vv and hh amplitude channels will have bursts of equal magnitude.

Figure 11 summarizes a description of scattering from mechanically-generated short gravity waves.

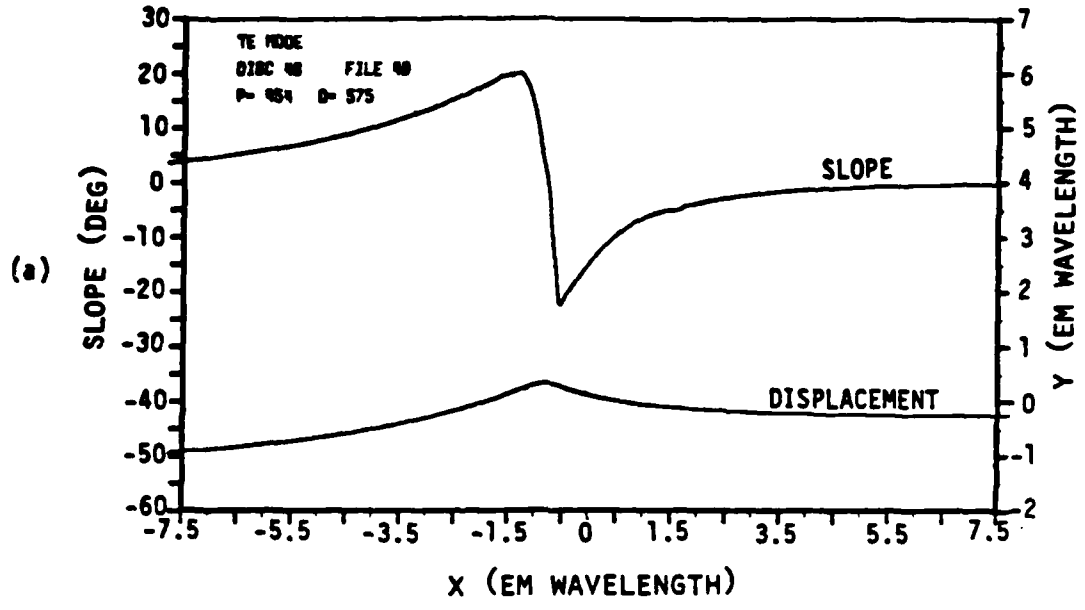

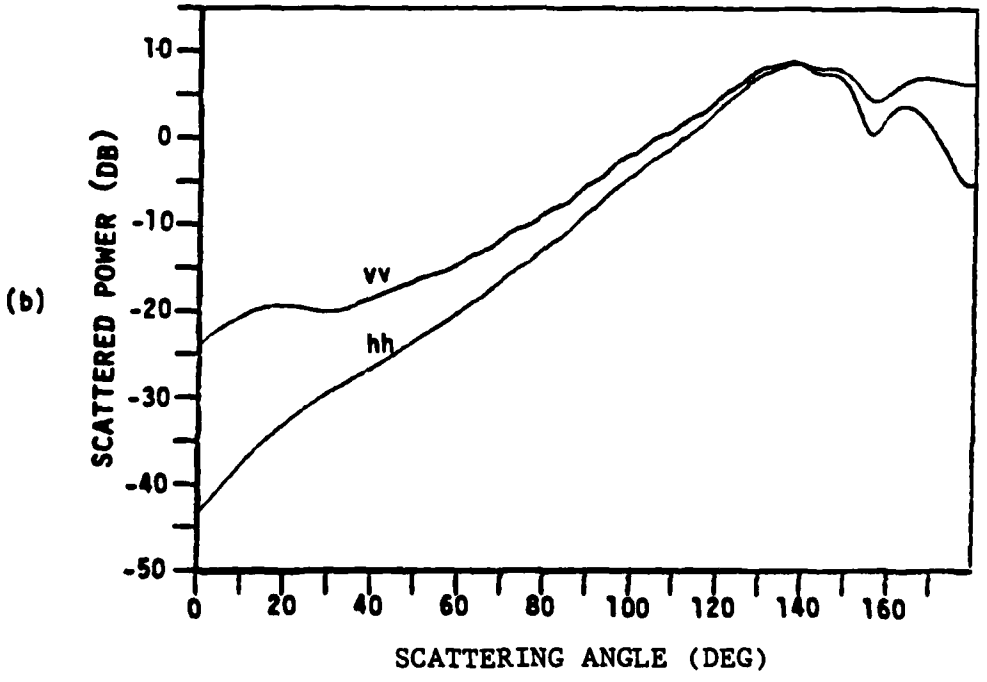

Figure 7. (a) Wave in Figure 3(a) with its capillaries smoothed away, leaving the "background wave form".
(b) Scattering from the "background wave form" as computed by the moments method for 67.7° incidence angle.

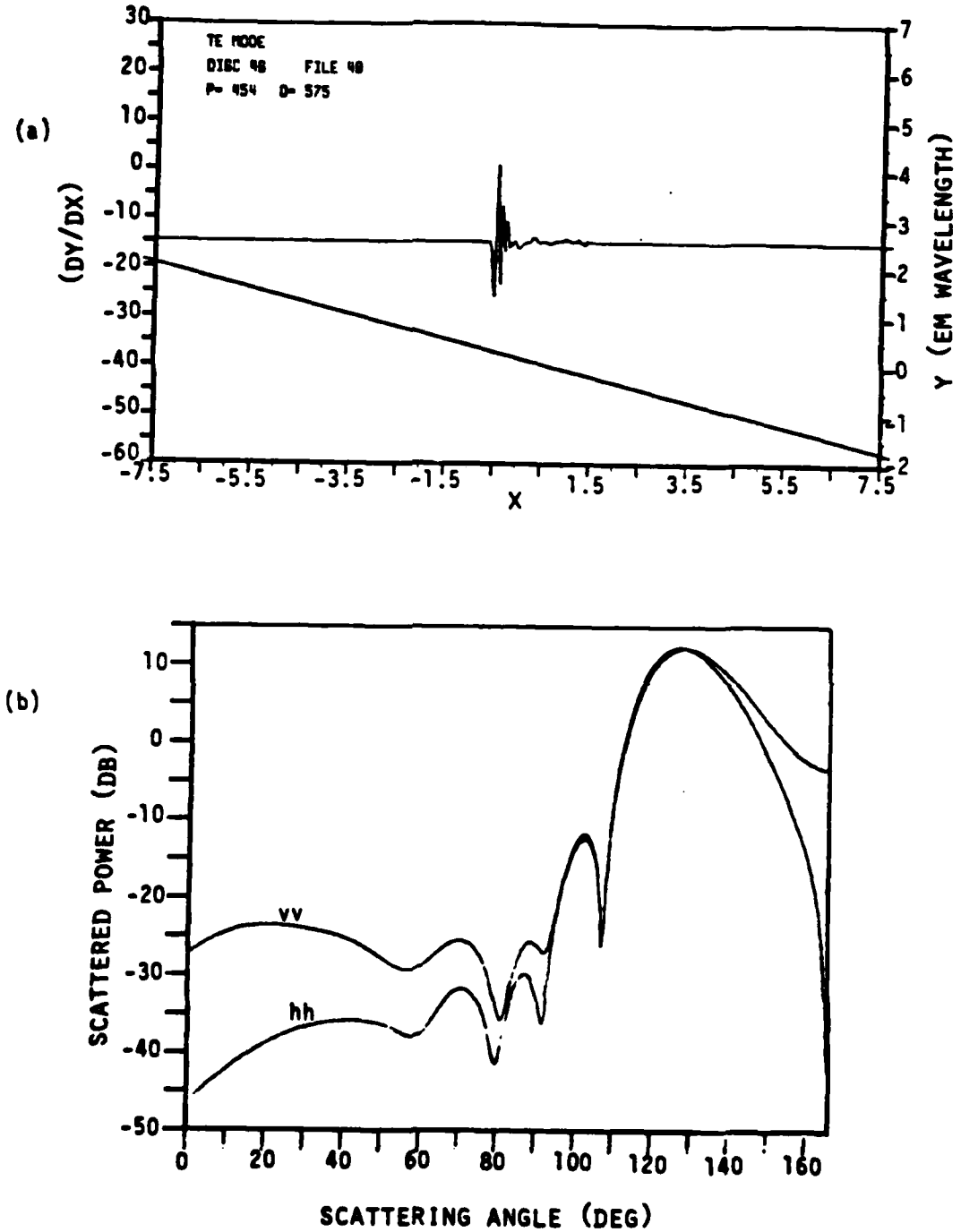

Figure 8. (a) The parasitic capillary wave of Figure 3 put on an inclined plane of 14.5°.
(b) Scattering from the parasitic capillary on an inclined plane as computed by moments method for 67.7° incidence plane.

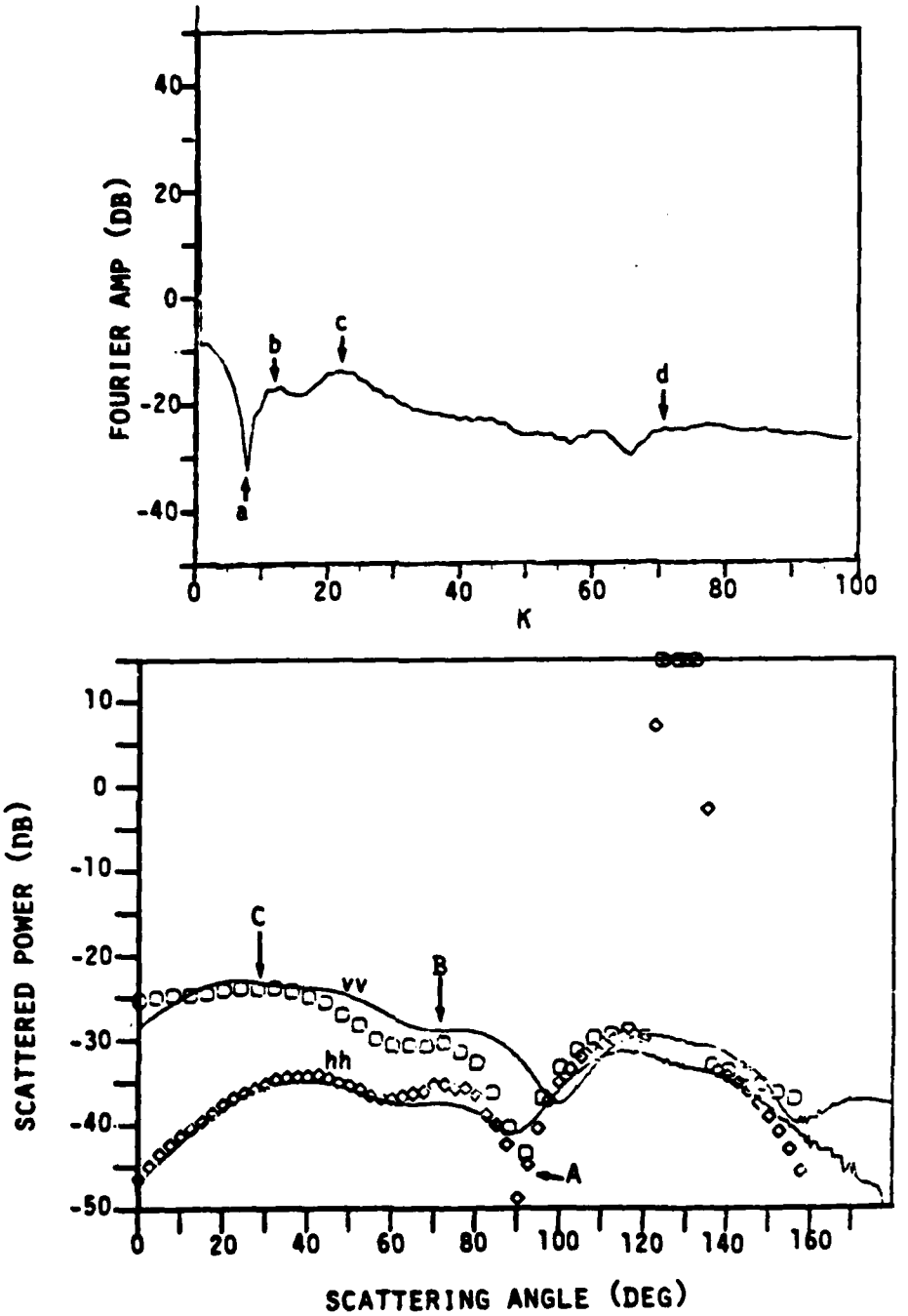

Figure 9. (a) Fourier spectrum of capillary waves of Fig. 8(a) on a horizontal plane. Horizontal axis $K \equiv k \cdot L/2\pi$ where $k \equiv$ wavenumber, $L \equiv$ range in $x = 15\ \lambda_e$.
(b) Symbols – scattering as computed by SPT for 67.7° incidence angle. Capillary waves are assumed to be on a 14.5° inclined plane. Solid lines – difference in scattering from original wave (Fig. 3) and scattering from "background wave form" (Fig. 7).

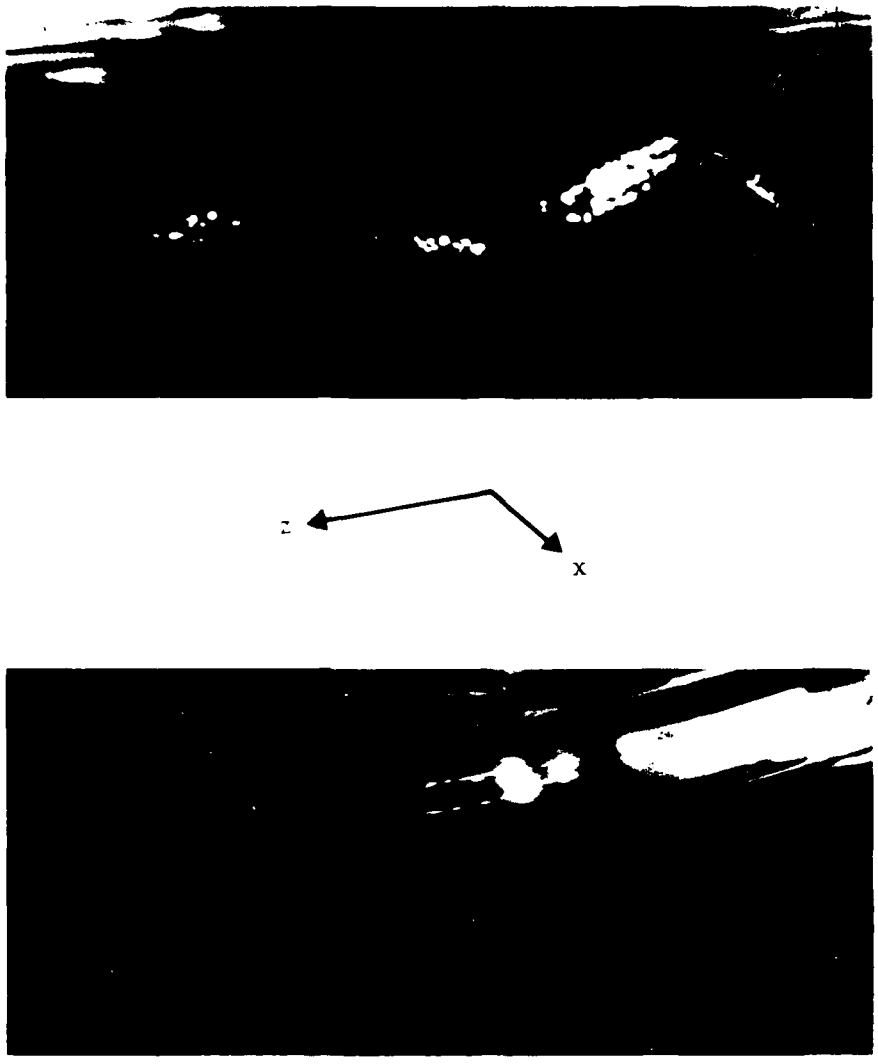

Figure 10. (a) Point-like specular facets at 55° incidence angle. This is typical for a highly turbulent wake.

(b) Ring-like specular facets at 55° incidence angle. This is typical of very steep capillary waves. The less steep oscillations of the capillaries can be seen in front. z is the cross-tank direction and x is the direction the waves are traveling. The lengths of $\vec{x}$ and $\vec{z}$ vectors represent 2 cm.

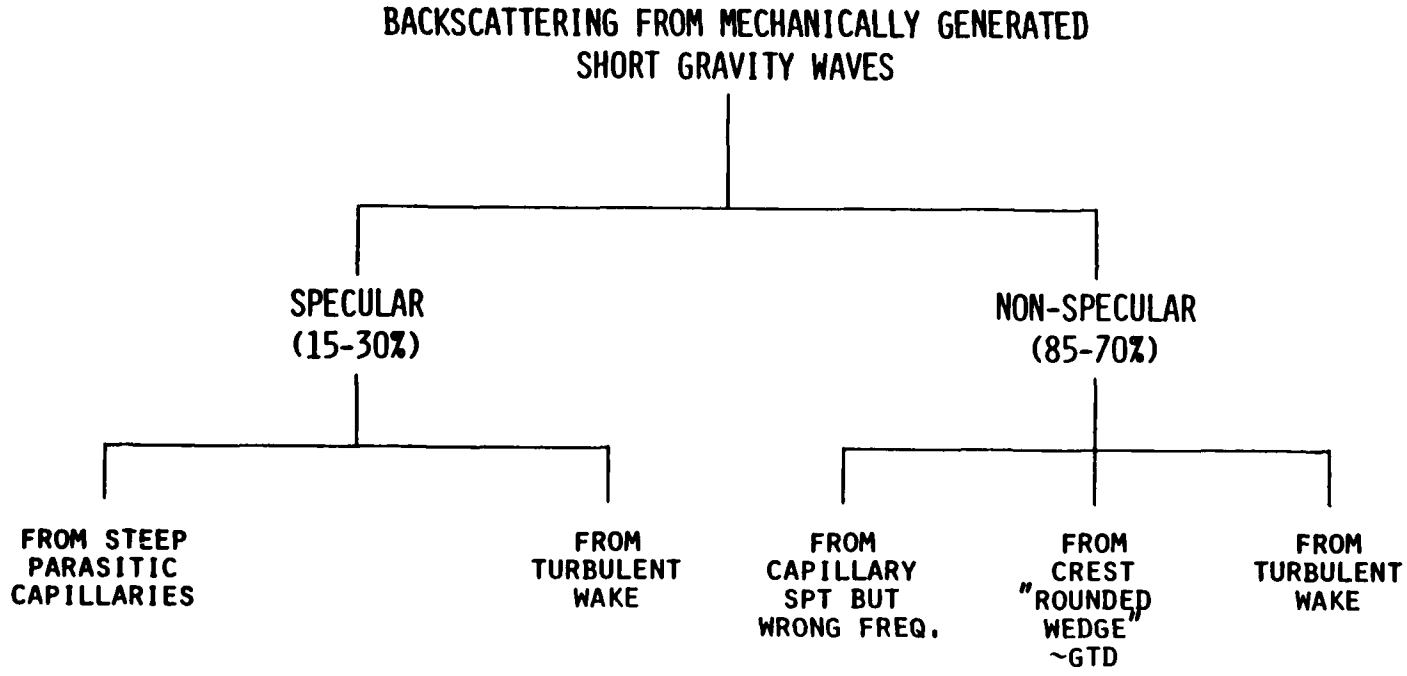
BACKSCATTERING FROM MECHANICALLY GENERATED
SHORT GRAVITY WAVES
SPECULAR
(15-30%)
NON-SPECULAR
(85-70%)
FROM STEEP
PARASITIC
CAPILLARIES
FROM
TURBULENT
WAKE
FROM
CAPILLARY
SPT BUT
WRONG FREQ.
FROM
CREST
"ROUNDED
WEDGE"
~GTD
FROM
TURBULENT
WAKE

Figure 11.

V. BACKSCATTERING FROM WIND-GENERATED WAVES

The Doppler spectrum of wind-wave scattering has been the subject of a large number of past studies. We are revisiting this area with a new point of view. The laser slope gauge provides us with information that enables us to understand the shape and evolution of the Doppler spectrum of the microwave backscatter as wind speed increases.

Figures 12(a), (b), (c), (d) show the spectrum in both polarizations from 2.5 m/s to 8.8 m/s wind speed at $\theta_i = 55°$. It can be seen that at low wind, the spectra in both vv and hh are narrow peaked, centered at about 16 Hz and have polarization ratios of ~ 11 db. At high wind, the spectra in both vv and hh are doubly peaked. The high frequency peak occurs at 30-40 Hz and has a polarization ratio of ~ 2-3 db. The lower frequency peak is broad and occurs at ~ 20 Hz, with a polarization ratio of ~ 8 to 10 db.

To understand the spectra, we have to look at the slope gauge recording. Figure 13(a) shows wind-wave scattering at 3.03 m/s. Figure 13(b) shows wind-wave scattering at 7.9 m/s. At low wind speed [Figure 13(a)], the scattering has the following characteristics: (i) The microwave amplitude has long-time duration compared with the dominant water wave period, implying that scattering may be associated with a large patch rather than with individual waves. (ii) The large polarization ratio (σ_{vv}/σ_{hh}) is evident. (iii) The phase channel shows uniform Doppler frequency. These observations strongly suggest that the water surface may indeed be "slightly rough" so that small perturbation theory is the correct approximate scattering theory. At high wind [Figure 13(b)] the scattering shows the following characteristics: (i) The slope gauge recording shows that there are two distinct kinds of features (a) rough patches, as in A and C in Figure 13(b), and (b) waves with parasitic capillaries, as in B in Figure 13(b). (ii) The rough patches are associated with large polarization ratio and small Doppler shift. (iii) The waves with capillaries are associated with a small polarization ratio and large Doppler shift. In the latter case the microwave amplitude also shows individual bursts corresponding to individual waves. The large polarization ratio associated with the rough patches suggests that the scattering may again best be described by small perturbation theory. The waves with capillaries look similar to the mechanically-generated self-modulating waves that we have studied, in which case there would be specular reflection from facets in

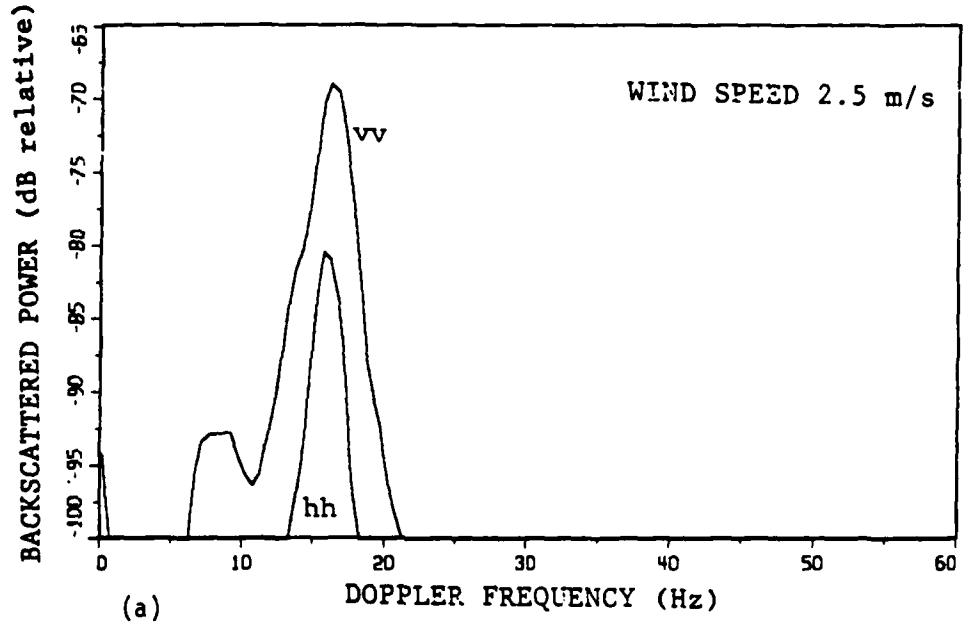

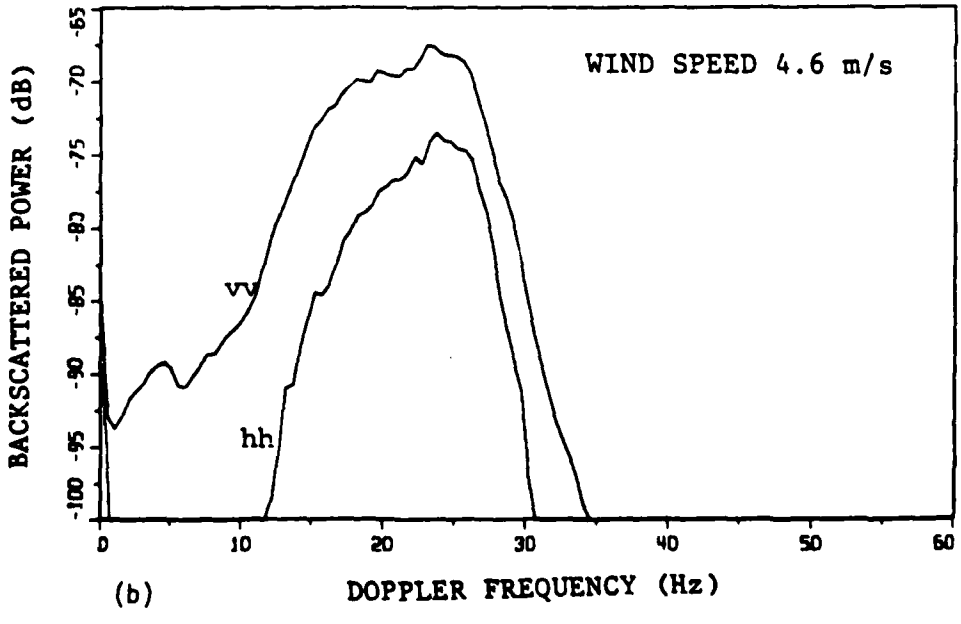

Figure 12. Wind-wave backscattering Doppler spectrum at $\theta_i = 55°$.

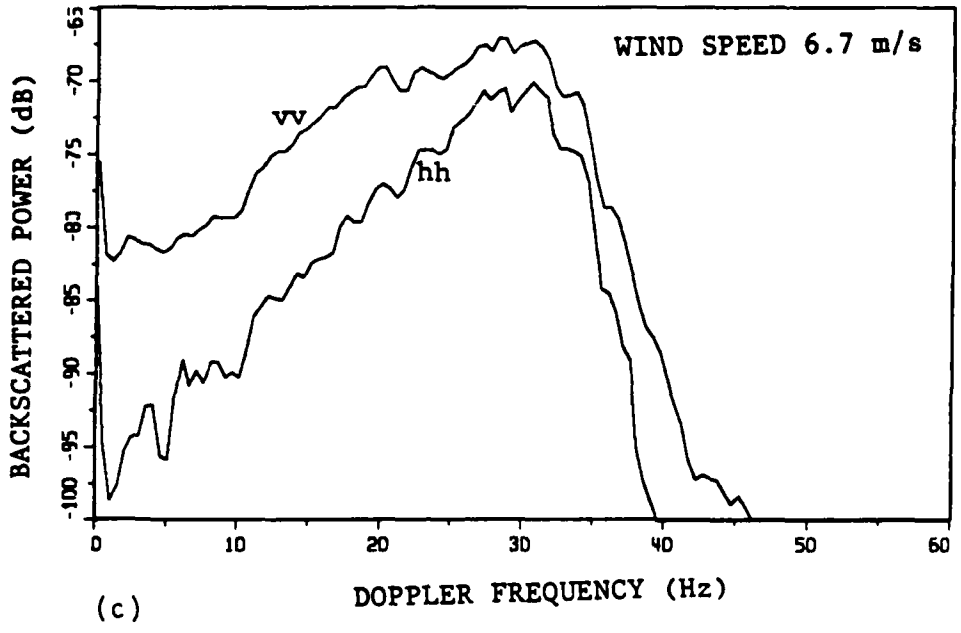

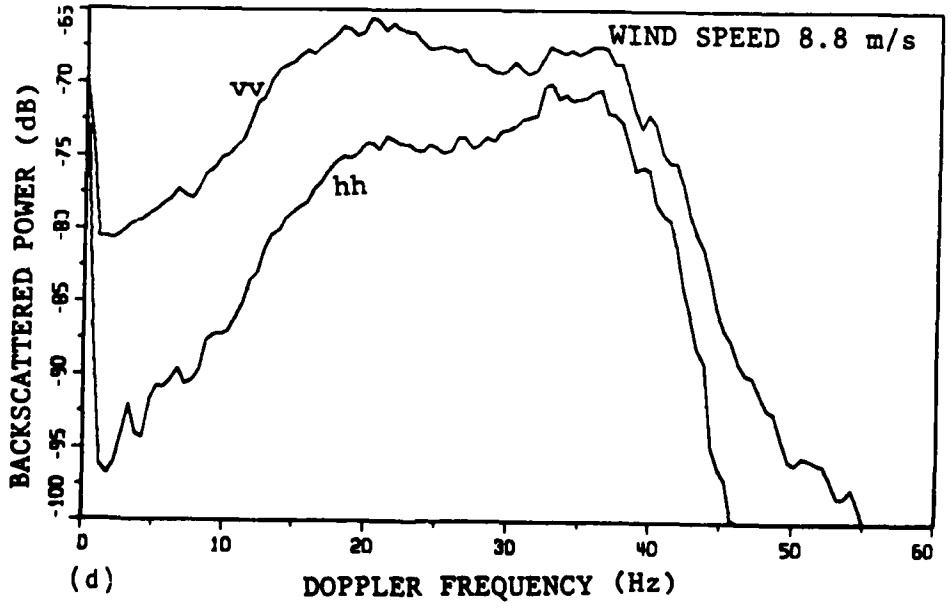

Figure 12. Wind-wave backscattering Doppler spectrum at $\theta_i = 55°$.

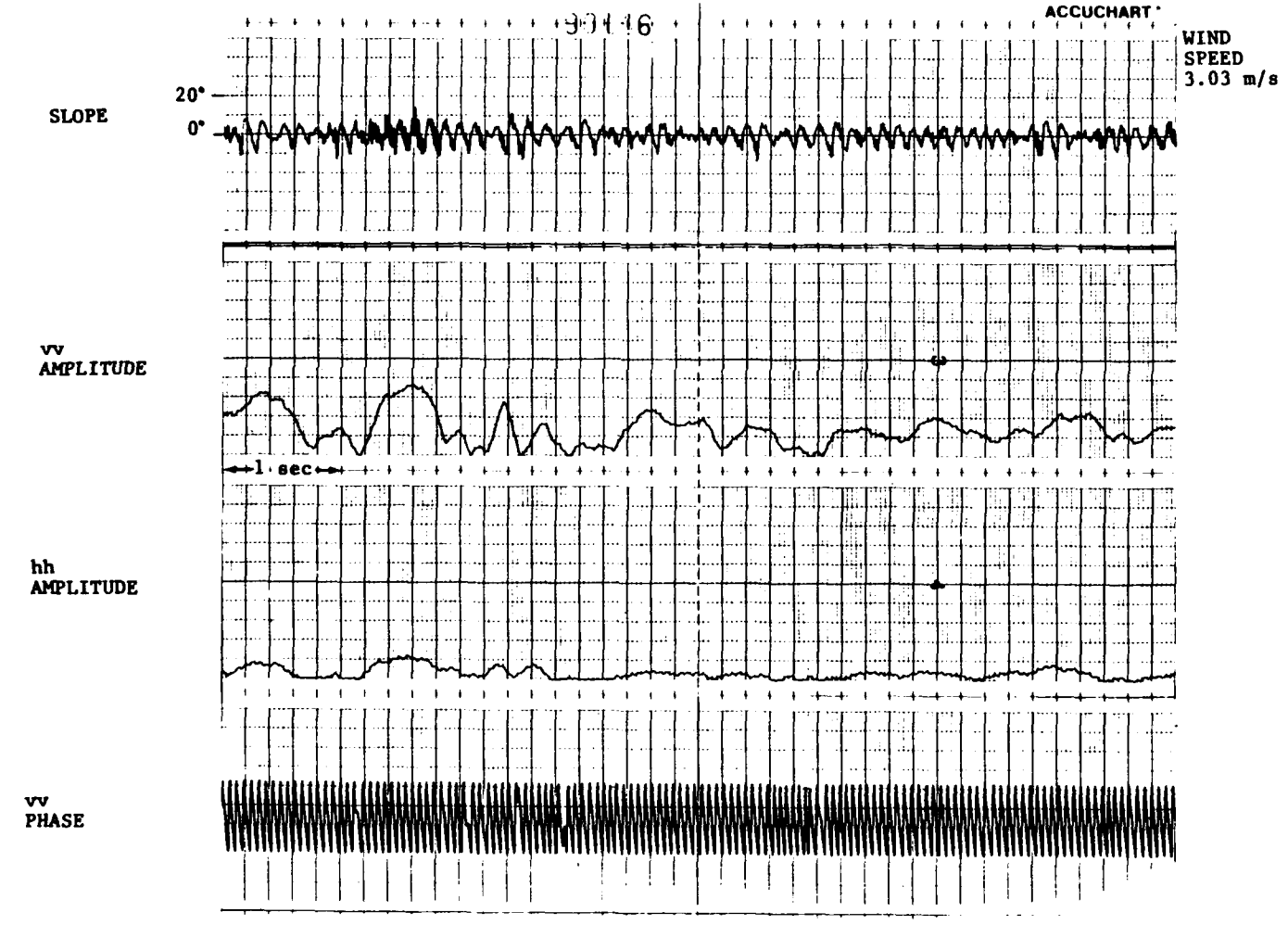
ACCUCHART
WIND
SPEED
3.03 m/s
SLOPE
20°
0°
VV
AMPLITUDE
1 sec
hh
AMPLITUDE
VV
PHASE

Figure 13(a)


WIND
SPEED
7.9 m/s
20°
0°
SLOPE
A
B
C
B
VV
AMPLITUDE
hh
AMPLITUDE
1 sec
VV
PHASE

Figure 13(b).

addition to wedge diffraction from crests and Bragg scattering from the capillaries. The large Doppler shift simply corresponds to the phase velocity of the dominant wave. Referring back to the Doppler spectrum in Figure 12, it is now evident that for low wind speed, the narrowness of the peak and the large polarization ratio of ~ 11 db are due to the fact that the water surface is "slightly rough" and Bragg scattering is the appropriate description. For high wind speed, the double peak in the spectrum suggests there are two distinct scattering features. The lower frequency peak with a large polarization ratio corresponds to scattering from the "rough patches", which again may be described as "Bragg scattering". The high frequency peak with a small polarization ratio corresponds to the "waves with parasitic capillaries", which scatters the microwave radiation by a combination of specular reflection, wedge diffraction and Bragg scattering.

The above offers a qualitative description for microwave scattering from wind waves. To confirm it in a more quantitative manner, we do the following. For low wind speed scattering, we perform sample calculations using the wave slope recording and the moments method. Using the same slope sample, we compute again, using the small perturbation theory. The results agree quite well, showing that the low wind surface is indeed a "slightly rough" surface so that the small perturbation theory is valid. The measured polarization ratio of ~ 11 db is exactly the value predicted by the small perturbation theory. The Doppler shift of about 16 Hz can be accounted for as the sum of the Bragg wave phase speed (11 Hz) plus a wind drift velocity (5 Hz = 3% of the wind speed). The picture is therefore a slightly wind ruffled surface composed of free waves traveling on a wind drift layer. By looking at the phase of the cross-spectrum between successive slope scans, the phase velocities of different frequency water wave components can be measured. The measured phase velocities confirm our picture.

At higher wind speed, the "rough patches" again scatter according to small perturbation theory. However, the Doppler shift of ~ 20 Hz is too low to be accounted for as a sum of Bragg wave phase speed plus wind drift velocity. Indeed, it is only slightly higher than the wind drift velocity. Relative to

the wind drift layer, the scatterers are almost staionary and have little intrinsic velocity of their own. This suggests turbulence. A measurement of the coherence of successive slope scans shows that the "rough patches" lose coherence much faster in this case than for the low wind speed surface.

For the "waves with capillaries" at high wind, measuring the phase of the cross-spectrum of successive slope scans shows that almost all the different frequency components travel at the same velocity as the dominant wave, i.e., we have a bound wave system. The large Doppler shift measured (30-40 Hz) simply corresponds to the phase velocity of the dominant wave.

The following table best summarizes the description for wind-wave scattering:

WIND-WAVE SCATTERING

LOW WIND	HIGH WIND	
EM: SPT HYDRO: FREE WAVES ON WIND DRIFT LAYER	<u>ROUGH PATCHES</u> EM: SPT HYDRO: TURBULENCE	<u>WAVES WITH CAPILLARIES</u> EM: SPECULAR FACETS CREST ∿ "ROUNDED WEDGES" CAP ∿ SPT HYDRO: BOUND WAVE

VI. CONCLUSIONS

Our conclusions regarding the nature of microwave backscatter from water waves based on these laboratory measurements can be summarized as follows:

1. Electromagnetically, we have identified three sources for microwave backscattering from water waves:
   - (i) specular reflection from turbulent wakes or steep capillaries
   - (ii) rounded wedge diffraction from sharp crests of waves
   - (iii) Bragg scattering from parasitic capillaries or turbulent patches.
2. Hydrodynamically, we have identified three sources for wind-wave scattering: low wind free waves, high wind bound waves and turbulent patches.
3. We now have explanations for
   - (i) the evolution of the Doppler spectrum with increasing wind
   - (ii) the width of the Doppler spectrum
   - (iii) the location of peak(s) of the Doppler spectrum
   - (iv) the asymmetry of the Doppler spectrum.
4. The implications for microwave backscattering from ocean waves are:
   - (i) specular reflection at low θ_i (e.g., 20°) may be much more important than generally expected
   - (ii) the relative frequency of occurrence of specular facets, sharp crests and turbulent patches will determine the character of ocean scattering, both for incident angle and frequency selection and for determination of modulation transfer functions.

REFERENCES

1. Rice, S. O., "Reflection of Electromagnetic Waves from Slightly Rough Surfaces," Comm. Pure Appl. Math. 4, 351-378.

2. Hasselmann, K., "Weak-Interaction Theory of Ocean Waves" in Basic Developments in Fluid Mechanics, ed. by M. Holt, Academic Press, N.Y., 1968.

3. Keller, W. C. and Wright, J. W., "Microwave Scattering and the Straining of Wind-Generated Waves," Radio Sci. 10, 139-147, 1975.

4. Chang, J. H. and Wagner, R., "Measurement of Capillary Wave Formation from Steep Gravity Waves," Paper presented at Conference on Atmospheric and Oceanic Waves and Stability of the American Met. Soc., March 29-April 2, Seattle, Washington, 1976.

DISTRIBUTION:

Office of Naval Research
800 North Quincy Street
Arlington, VA 22217
Attn: Mr. Hans Dolezalek, Code 422CS

1 Copy

Office of Naval Research
Western Regional Office
1030 East Green Street
Pasadena, CA 91106

1 Copy

Administrative Contracting
Officer (ResRep, DCASMA)

1 Copy

Director, Naval Research Laboratory
Attn: Code 2627
Washington, D.C. 20375

6 Copies

Defense Technical Information Center
Bldg. 5, Cameron Sta.
Alexandria, VA 22314

12 Copies

Robert C. Beal
APL/JHU
Johns Hopkins Road
Laurel, MD 20707

Dr. Wolfgang Boerner
University of Illinois at
Chicago Circle
Chicago, Illinois

Rod R. Buntzen
Code 1603, NOSC
San Diego, CA 92151

Prof. Dr. Klaus Hasselmann
Max Planck Institut f. Meteorologie
Bundes Strasse 55
D-2000 Hamburg 13
West Germany

Dr. D. W. S. Lodge
Remote Sensing Applications &
Research Station
Procurement Executive, Ministry
of Defense, Royal Aircraft
Establishment, Space Department
Farnborough, Hampshire
England

Dr. Richard K. Moore
The University of Kansas Center
for Research, Inc.
2291 Irving Hill Drive, Campus West
Lawrence, KS 66045

Dr. William Plant
Code 4305
Naval Research Laboratory
Washington, D.C. 20375

Dr. Keith Raney
Canadian Center for Remote Sensing
2464 Sheffield Road
Ottawa, Ontario, K1A OY7
Canada

Dr. Omar H. Shemdin
Jet Propulsion Laboratory
4800 Oak Grove Drive
Pasadena, CA 91130

Dr. Robert A. Shuchman
Manager, Radio Remote Sensing Program
Environmental Research Institute of
Michigan
P.O. Box 8618
Ann Arbor, Michigan 48107

Dr. Gordon Smith
APL/JHU
Johns Hopkins Road
Laurel, MD 20707

Dr. Dennis B. Trizna
Code 5320
Naval Research Laboratory
Washington, D.C. 20375

Dr. Gaspar R. Valenzuela
Code 4305
Naval Research Laboratory
Washington, D.C. 20375